



Original Research Article

Efficiency of Different Physical Surface Modalities on Osseointegration of Titanium Alloy Implants

Enas M. Eldadamony, Nadia A. Badr, Enas M. Hegazy, Hoda A Fansa, Ibrahim E. Helal

¹Lecturer of Dental Materials, Faculty of Dentistry, Suez Canal University.

²Professor of Dental Biomaterials, Faculty of Oral & Dental Medicine, Cairo University, Affiliated to Faculty of Dentistry, Umm Al-Qura University.

³Lecturer of Oral Biology, Faculty of Dentistry, Suez Canal University.

⁴Lecturer of Oral Biology, Faculty of Dentistry, Alexandria University.

⁵Assistant Professor, Surgery Department, Faculty of Veterinary Medicine, Suez Canal University.

Corresponding Author: Nadia A. Badr

Received: 17/03/2015

Revised: 16/04/2015

Accepted: 21/04/2015

ABSTRACT

Aim: To investigate the effect of physical surface treatments; plasma immersion nitrogen ion implantation (PIII) and Nd:YAG laser, on topographical morphology and texture of Ti-alloy implants and consequently their osseointegration.

Materials & Methods: Fifteen Ti-6%Al-4%V cylindrical root shaped samples were divided into three groups. Group I (Control): received no surface treatment, Group II: treated by PIII and Group III: subjected to Nd:YAG laser.

The sterilized implants were inserted into Mongrel dogs' femur for 6 months before animals scarification. Implants within bone blocks were used for histological assessment of the newly formed bone. For histomorphometric analysis, bone-to-implant contact (BIC %) was calculated. The collected data were statistically analyzed.

Results: SEM of Group I showed regular parallel lines of cutting and polishing. Group II showed parallel homogenous strai of highly polished surface. Group III exhibited sealed machining and polishing marks due to laser heating with uniform irregularities disturbed by tiny pores. Surface roughness of Group III recorded the highest significant mean value ($168.24 \pm 13.00 \mu\text{m}$) while Group I recorded the least significant mean value ($114.32 \pm 6.74 \mu\text{m}$). Group II recorded an intermediate significant mean value ($126.94 \pm 10.92 \mu\text{m}$).

Histologically, Group I showed fibrous tissue interposition at bone/implant interface with chronic inflammatory cells. Meanwhile, Group II & Group III showed an intimate bone-to-implant contact with mature bone formation. BIC% followed the same significant rank of surface roughness: Nd:YAG ($84.62 \pm 5.05\%$), followed by PIII ($64.60 \pm 3.27\%$) while control group ($23.78 \pm 2.71\%$).

Conclusion: Physical surface modalities; PIII and Nd:YAG laser, yielded an effective surface topography of Ti-implants that enhanced their osseointegration.

Key words: Surface treatment, Ti-alloy implants, Plasma Immersion Ion Implantation (PIII), Nd:YAG laser, Osseointegration.

INTRODUCTION

Modern dentistry goal is to restore the patient to normal function, speech, health and aesthetics, regardless of the atrophy, disease or injury of the stomatognathic system. Responding to this ultimate goal, dental implants are an ideal option for people in good general oral health who have lost from one tooth up to a whole arch or even to stabilize a moving denture offering a successful alternative to many restorative problems. ⁽¹⁾

Dental and orthopedic implants have been under continuous advancement to improve their interactions with bone and ensure a successful outcome for patients. The confirmed outstanding effects of surface characteristics such as topography and chemistry can serve as design tools to enhance the biological response around the implant. ⁽²⁾ Surface treatments and coatings accomplished by different techniques have been developed in order to provide a micrometrical roughness akin to the size of bone cells, to guarantee the best possible osseointegration, anchorage and stability. In this sense, the best candidates to be used as biomaterials are titanium and its alloys. ⁽³⁾

Osseointegration has been defined as a direct structural connection at the light microscopic level between bone and the surface of a load-carrying implant. ⁽⁴⁾ No soft connective tissue or periodontal ligament-like interface is detectable between the bone and the implant, and the osseointegrated implant functions without mobility. ⁽⁵⁾

The rate and quality of osseointegration in titanium implants are related to their topographical properties. Surface composition, hydrophilicity and roughness are parameters that play a role in implant-tissue interaction and osseointegration. The chemical composition or charges on the surface of titanium implants; which are important for protein

adsorption and cell attachment, differ depending on bulk composition and surface treatments. ⁽⁶⁾

Owing to different surface modalities, thorough identification of implant topography is a crucial issue need to be addressed. Hence, this study was aimed at surface treatments of Ti-implants by plasma immersion nitrogen ion implantation (PIII) and Nd-YAG laser in a trial to enhance their osseointegration after insertion in the femurs of Mongrel dogs.

MATERIALS & METHODS

Ti-6%Al-4%V alloy supplied by Central Metallurgical Research Institute (CMRDI), Cairo, Egypt; was presented as a rod and cut into cylinders equal in length using wire cutting machine (CUTO 20-JEANWIRITZ, Germany). A total of fifteen cylindrical root-form shape samples of diameter 4 ± 0.2 mm and 11 ± 0.4 mm lengths were obtained.

The cut samples were polished mirror-like using Emery paper starting from grit #600 up to #1200 to remove surface macro-defects. Afterward, they were washed with 70 vol% ethanol at room temperature, cleaned ultrasonically (JULBO, LABORTEVHNIK GMBH, Germany) in distilled water for 5 minutes and then dried by air drier (BRAUN, Germany). The samples were divided into three groups; (n=5), according to the received surface treatment. Group I: samples were kept without any surface treatment to serve as control, Group II: samples treated by plasma immersion nitrogen ion implantation (PIII) and Group III: samples were subjected to Nd:YAG laser application.

The samples of Group II were surface treated at Plasma Center, Department of Physics, Faculty of Science, Azhar University. The plasma focus device was energized by a condenser bank of 30 μ F (micro Faraday) capacitance, 27 nH (nano

Henry) inductance and maximum potential of about 15 KV (3.3 KJ). The condenser bank was charged to the applied voltage using variable high voltage charger DC power supply. The electrodes system consisted of an anode of 16 cm long hollow copper tube of 1.9 cm diameter (central electrode) surrounded by six 1 cm thick copper rods of 16 cm long forming the cathode. The electrodes system is enclosed in glass vacuum chamber of 16 cm diameter and 35 cm long. The vacuum was provided by a single stage rotary pump recharged by pressure of about 0.005 torr. The sample holder was positioned in the vacuum chamber facing the rim of the anode.

The selected working gas; nitrogen (N_2), was charged in a condenser bank up to a potential difference of 12 KV which was in turn transformed to plasma focus tube through air spark gap. In this state, the plasma focus was formed due to dissociation into ions and electron beams; the energetic nitrogen ion beam took the shape of fountain and spread upwards to bombard the facing samples. This process is repeated for 15 times to ensure adequate and uniform surface treatment of the sample. ⁽⁷⁾

The samples of Group III were surface treated using pulsed Nd: YAG laser (Continuum Surelite, National institute of laser enhanced sciences, Cairo University). The laser surface treatment was carried out with 1.064 nm wavelength (λ) irradiation, at a pulse frequency of 20 to 35 kHz (ν), scanning speed ranging between 80 and 300 mm/s and at scanning space from 0.1 to 0.2 mm/s. Laser interval was 300 ns with energy 200 mJ/pulse. ⁽⁸⁾ Laser scanning velocity was kept constant by a precise adjustable XYZ translator. ⁽⁹⁾ The sample was mounted on a specially designed revolving motor such that ensure complete lasing of the surfaces. Each sample was subjected to the laser beam for one minute.

Characterization of Ti- alloy sample surface:

Scanning Electron Microscope (SEM, JEOL JSM 5410 -Japan) was used to examine surface morphology of representative samples for each group. Meanwhile, Environmental scanning electron microscopy (ESEM, Quanta 200, FEI,-Multinational gathered at Netherlands) determined the surface roughness. By the aid of special software (XT document, x-ray tungsten filament document for microanalysis measurements), an area was specified and converted into 3-D images corresponded to the texture of the traced surface.

Finally, prior to surgical procedure, it was mandatory to sterilize the samples by exposure to a specific γ - radiation sterilization dose of 2.5 mega rad in the range of 1.0023 KGY/hr (60 Co, Baha, Baha Indian Cobalt- 60-4000A, National Center for Radiation Research and Technology NCRRT, Cairo, Egypt). ^(10,11) Then, they were kept in sterile package till usage in a veterinary theatre at the Department of Surgery, Anesthesiology and Radiology, Faculty of Veterinary Medicine, Suez Canal University, Egypt in accordance to the approved regulations of the Institutional Ethical Committee.

Surgical procedures:

Five adult male Mongrel dogs with an average age 22 ± 2 months old and weighing 15-18 kg were used in this study. The dogs were fasted for 12 hours and premedicated with intramuscular injection (I.M.) of chlorpromazine hydrochloride in a dose of 1 mg/kg, 15 min prior to the induction of general anesthesia. ⁽¹²⁾ The skin was washed with soap and water followed by disinfection with chlorhexidine-alcohol. The surgical site was clipped, shaved and then cotton surgical scrubs wetted with Betadine (Povidone-Iodine U.S.P. 10%, El Nile-Co.) were applied for ten minutes.

Finally, general anesthesia was conducted by intravenous injection of thiopental sodium 2.5%, 500mg (Egyptian INT. pharmaceutical industries Co., E.I.P.I.C.O.)

The right femur was completely exposed by a lateral skin incision and blunt dissection of the muscles. ⁽¹³⁾ A size 4 rose round head bur was used to locate and initially perforate the implant site with low speed and saline coolant. The hole was extended through the cortex into cancellous bone. Three adjacent implant beds with appropriate distance among them were prepared using a progressive sequence of spiral drills (Superline, Implantium Company, UK). The drilling procedures were performed at speeds less than 1500 rpm under copious irrigation of sterile saline to reduce the risk of thermal bone damage due to overheating. The initial drilling was performed by 2 mm diameter pilot drill at 1200 rpm; then, slower speed of 800 rpm for sequential drilling with burs of 2.5, 3.0, 3.5 mm. The implants sites were prepared to a depth of 11 mm such that they were parallel to each other to individually facilitate sectioning of each implant later. At the end, the implants were carefully handled to avoid contact contamination. They were press fit into the osteotomy sites by manual light pressure and with a regular up-and-down motion in order to maximize access of the saline to the full depths of the implant hole to wash bone debris. A balanced electrolyte solution (0.9% Sodium chloride: I.V. infusion B.P.2000, ElNasr pharmaceutical chemicals co. Adwia, Egypt) was administered in amount of 10 ml/kg/hr throughout surgical procedures.

The fascia-periosteum were closed individually with single resorbable sutures (Coated Polyglycolic acid PGA; Ethicon, Germany) No.1. Vastus lateralis and the biceps femoris muscles were sutured together with a simple continuous suture pattern. As well, sub-cutaneous tissues was

sutured following the same pattern while the skin was sutured with an interrupted horizontal mattress suture pattern using non absorbable suture material (D-tek) (Demophorius limited, Cyprus.) No.1.

Each experimental animal was injected postoperatively with 1g of amoxicillin (I.M.) (E.Mox: Egyptian International Pharm. Industries Company, Egypt) and dipyrone in a dose of 10 mg/kg I.M. for 5 days (Analgin 50%: El-Nasr pharmaceutical Chemicals Co., Egypt.). Every dog was set aside in separate cage and allowed for water free choice till gradually returned to full feed over the next 48 hours. They were inspected few days postoperatively for signs of wound dehiscence or infection, any abnormal swelling or discharges. The surgical stitches were removed 10 days postoperatively.

After 6 months, the experimental animals were sacrificed by an over dose of thiopental. The skin was reopened and the bone with the implant was removed as block and immersed in formalin. The specimens were dissected and fixed in 10% formal saline for 48 h.

Assessment of the newly formed bone:

Histological Study:

The formalin-fixed, tissue-implant blocks were dehydrated in a graded series of ethanol and embedded in acrylic resin prior to cutting along the long axis of the implant and through the surrounding bone using a diamond saw (IsoMet 4000 precision microsaw Buehler, USA.). The cut sections were ground until specimens of 150 μ m thickness were obtained, then, stained with haematoxlin and eosin (H&E) and examined under optical light microscope at magnification X 40.

Histomorphometric Analysis:

Bone-to-implant contact (BIC) is a histologic concept assessed by calculating the implant surface area directly attached to mineralized bone without soft connective

tissue interposition. BIC ratio provides a valuable osteoconductive index.

SEM at low magnifications (X20) was used to analyze CIB histomorphometrically using free software (Image J 1.48 v, Wayne Rasband, National Institute of Health, USA.). BIC was determined by linear measurement of direct bone contact with the implant surface. The sum of the lengths of the bone formation on the implant surface in the cancellous and cortical bones to the total implant length is the bone implant contact ratio. (14-16) The sites were standardized in all implants at both sides and bottom of implant. All measurements were determined and expressed as percentages of osseous tissue contact at the designated perimeter of each implant as follow.

$$\%BIC = \frac{\text{Sum of the length of the part of bone formation on the implant surface (green line)}}{\text{Total implant length (red line)}} \times 100$$

Statistical Analysis:

The collected data were analyzed by SPSS version 16. One Way Analysis of Variance (ANOVA) test compared the investigated groups; then, Post-hoc statistical test was considered significant at

95% level of confidence. P-value was < 0.05 between every group and control group and between PIII group and laser group.

RESULTS

Surface Characterization:

SEM Examination:

SE micrograph of Group I shows a closely related microstructure to the cutting tool consists of regular pattern of shallow grooves; Figure 1-A. Machining created typical microscopic grooves and relatively smooth surface characteristics. The polishing marks appeared as parallel lines crossed by scratches. The surface morphology of Group II; Figure 1-B, shows an obvious homogenous ultra-microstructure surface with very fine parallel striae of the highly polished surface. Meanwhile, scratches of machining and polishing of Group III; Figure 1-C, are sealed due to direct laser surface heating. A uniform appearance of surface roughness was characterized by deep and regular morphological pattern with tiny pores. The laser re-molten surface has brushed appearance disturbed by defined pore pattern.

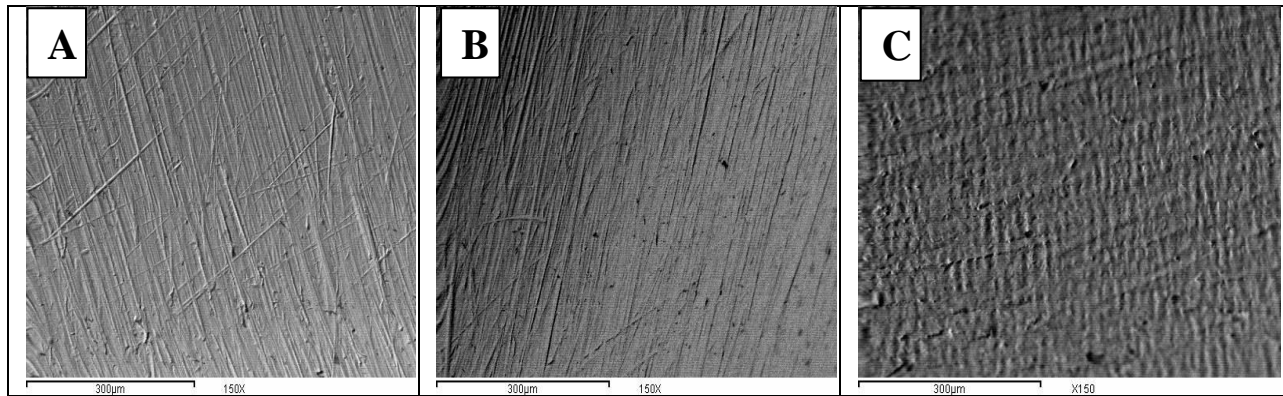


Figure (1): SE Micrographs of Groups I (A), Groups II (B) and Groups III (C) at magnifications X150

Environmental Scanning Electron Microscopy:

Table1 shows the mean surface roughness (Ra) values of the investigated groups in (µm).

Fig.(2) shows ESEM of the tested groups. The 3D surface texture of Group I; Fig. 2-A, shows short non prominent elevations with rounded tips. Fig. 2-B reveals shag appearance 3D surface texture of Group II. There are slight prominent peaks with fine and shallow pores are uniformly speckled

among them. On the other hand, Fig. 2-C exhibits 3D surface texture of Group III where high peaks are prominent and many of them are truncated. Deep valleys are regularly scattered among their elevated prominent tips.

Table 1: The mean values, standard deviation (SD) values and results of ANOVA test of surface roughness values (Ra) in (µm) of the surface treated groups

Group	Roughness		
	Maximum	Minimum	Mean
Control	126.82	109.05	114.32±6.74 ^c
Plasma immersion ion implantation	143.21	111.29	126.94±10.92 ^b
Nd:YAG Laser treatment	194.56	157.02	168.24±13.00 ^a

Means with different letter within each measurement are significantly different at p=0.05.

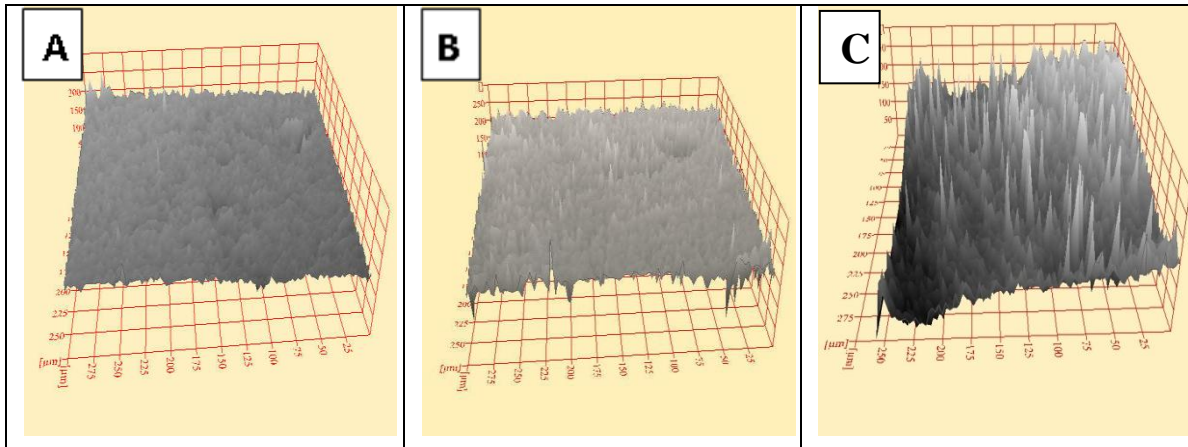


Figure (2): ESE Micrographs of topographical texture of Groups I (A), Groups II (B) and Groups III (C)

Assessment of Osseointegration:

Histological Examination:

Group I; (Fig.3-A), showed peri-implant fibrous tissue directly against the implant surface at implant/ bone interface. There are obvious mild to moderate chronic inflammatory cells infiltration (black arrow) and tiny vascular spaces (arrowhead). No sign of new bone formation was observed.

Group II; (Fig.3-B), showed peri-implant tissues of mature lamellar bone formation at the implant/ bone interface with mature osteocytes in direct contact with the implant

surface. No inflammatory reactions were recognized.

Group III; (Fig.3-C), showed peri-implant tissues of mature well organized compact bone is in direct contact with the implant surface. This bone covered the implant surface and appeared well osseointegrated. Small Haversian canals with blood vessels are evident. Abundant osteocytes with their characteristic stellate shape and their lacunae were found. Fibrous connective tissue was not present at the bone implant interface and no evidence of inflammatory cells.

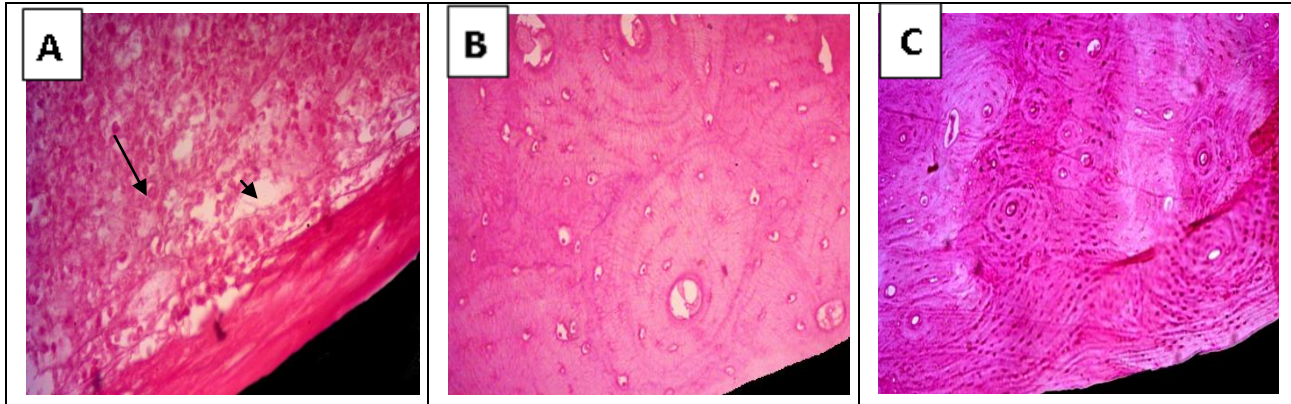


Figure 3: Photomicrographs of the histological structure of the peri-implant tissues of Groups I (A), Groups II (B) and Groups III (C), (H&E X40)

Histomorphometric Analysis:

The Bone/implant contact percentage (BIC %):

Table 2 shows bone-implant contact percentage (BIC %) of the tested groups and Figure 4 are representative samples of the tested groups.

Table 2: Mean; standard deviation (SD) values and results of ANOVA test of (BIC %) of the tested groups

Groups	(BIC%)± SD
Control	23.78±2.71 ^c
Plasma immersion ion implantation	64.60±3.27 ^b
Nd:YAG laser	84.62±5.05 ^a

Means with different letter within each measurement are significantly different at p=0.05.

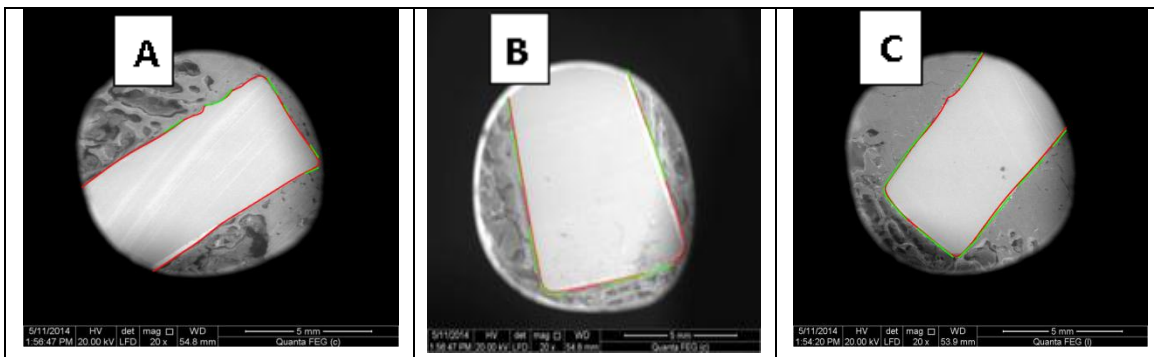


Figure 4: SE Micrographs show the BIC% of Groups I (A), Groups II (B) and Groups III (C) at magnification X 20

DISCUSSION

There is an interest in reducing the healing time after surgery and loading the implants with oral forces safely. In order to shorten the healing time, one of the strategies is to alter the biocompatibility of titanium implant surfaces to enhance bone formation in the peri-implant region. (17) Titanium is a bioinert nonbonding material to bone; therefore, approaches have mainly focused on enhancing the bioactivity of titanium and providing a higher

osteoconductivity to the bulk material by surface modifications. Surface chemistry modifications of the implant material and increase of the 3D surface area initially influence the binding capacity of fibrin and the release of growth factors, (18) Thus, the goal of the employed surface treatments was to alter the surface chemistry and texture. Consequently, promote the biological response and the osseointegration for the fixation and the stability of the implant.

Surface Treatment:

Plasma surface modification is possible to change not only the chemical composition and properties but also the biocompatibility of materials surfaces can be enhanced. ⁽¹⁹⁾ Plasma immersion ion implantation can modify the surface without altering the bulk properties of the implants material. ⁽²⁰⁾

A nitrogen gas was selected to modify the biomaterials surface by the formation of a nitride layer. Earlier studies indicated that plasma nitriding is capable of improving cell adhesion by changing surface roughness and wettability; ⁽²¹⁾ indicated that PIII provided nitrogen-rich and more hydrophilic surface that improve the biocompatibility of Ti implants without changing its surface morphology, Fig2-B.

The process was adequately applied for 15 repeated times to ensure uniform, dense and pinhole free coatings of the samples' surface yielding an increased surface energy and reactivity for excellent interfacial bonds ⁽²²⁾ and an increased surface area and roughness. ⁽²³⁾ The resultant surface roughness of plasma treated was significantly slightly higher ($126.94 \pm 10.92 \mu\text{m}$) than the control group ($114.32 \pm 6.74 \mu\text{m}$).

It is relevant to mention that optimizing the Nd:YAG laser process parameters was essential to form a defect free and continuous surface layer. Laser parameters determine the maximum temperature attained, the cooling rate and the duration determine the interaction among phases. As the heating and cooling rates are very rapid, a refined microstructure affects the surface mechanical properties significantly ⁽²⁴⁾ but not deteriorate the bulk mechanical properties. ⁽²⁵⁾ Thus, one minute duration was selected to produce ultra-structural changes in the oxide layer.

Better osseointegration due to laser treatment might interpret for an improved

bone response because of the produced ideal pores with a specific diameter and depth. *Itala et al, 2000* ⁽²⁶⁾ reported that optimal roughness from 100-400 μm ; Table1& Fig. 2-C, is needed to encourage the mineralized bone. ⁽²⁷⁾

Surface Characterization:

A rough topography obviously increases the surface area of the implant adjacent to the bone and improves cell adhesion to the surface, thus; achieves higher bone-to-implant contact and better biomechanical integrity. ⁽²⁸⁾ Roughened surface would render nonbonding biomaterials into bone-bonding and improve the interfacial retaining mechanics. ⁽²⁹⁾ In agreement with numerous studies, ^(6,28) the increased surface roughness of the dental implants enhances osseointegration compared to smoother ones. However, systematic reviews and Cochrane collaboration ^(30,31) were not able to find any clinical evidence supporting the positive effect of increasing surface roughness on osseointegration.

The role of the roughened surface is complex since the actual strength of bone contact is quite low (4 MPa or less) resembling those of electropolished surfaces; however, the latter showed little bone contact ^(32,33) suggested that high surface roughness alone is not the only criteria to consider for optimal osseointegration. The pattern, size, and distribution of peaks and valleys that compose the surface texture may significantly influence the overall intimacy and mechanical interlocking of the bone-implant interface. ⁽³⁴⁾

Osseointegration Assessment:

In this study, dog was the experimental animals' model of choice for preclinical trials of surface treated implants. Scientists cited that about 85% of genes in dogs have a human equivalent. Three weeks to three years of experimental studies in the

dog contrasts sharply with the duration of human clinical use and of post-mortem retrievals ranged from 5 to 21 years, respectively. ⁽³⁵⁾

It is well established that characteristics of the implants' surfaces such as nano- and micro-topography, physicochemical composition and crystal structure have a major influence on the outcome of osseointegration, especially at the histological level. ⁽³⁶⁾ The interactions occur mostly between the host bones and the titanium implant at the interface in a living body depend mainly upon the implant's surface characteristics per se. ^(37,38)

Despite, the clinical assessment of osseointegration is based on mechanical stability; primary and/or secondary, ⁽³⁹⁾ the biological stability is achieved by osteogenesis. Osteogenesis in a peri-implant environment results from two distinct mechanisms. Distance osteogenesis occurs when bone matrix is deposited from the host bone towards the implant surface. Contact osteogenesis occurs when bone matrix is deposited from the implant surface to the host bone. This is due to a complex cascade of events that characterize the early peri-implant healing period, in which osteoconduction and de novo bone formation are the key mechanisms. ⁽⁴⁰⁾ The osteoconduction is influenced by and dependent upon the implant surface while, the process of bone formation itself is independent of the surface material.

Comparing the histologic results in this study, bone regeneration process was observed by formation of mature compact bone in direct contact with the implant surface with no sign of bone resorption in both Groups II&III. On the other hand, Group I showed fibrous tissue interposed at the implant/bone interface with chronic inflammatory cells and tiny vascular spaces. Experimental evidence from in vitro and in vivo studies strongly suggests that some

types of surface modifications promote a more rapid bone formation than machined surfaces. Because osteoblasts are located on the surface of the titanium implant, surface roughness affects the synthesis of biological factors by osteoblasts and modulates the tissue response at the interface between bone and implant. ⁽⁴¹⁾ It was reported that a rough titanium surface stimulates the local production of PGE 2 and TGF- B_1 . This would interpret for the histological findings exhibited by the investigated surface treated titanium implants.

The formation of lamellar compact bone with Haversian systems due to osteoblastic proliferation and differentiation in vivo without abrupt changes of surface morphology as those specimens treated with PIII; Figure 3-B, was in coincidence with the findings of. ⁽²¹⁾ The laser treated samples showed signs of bone remodeling in form of well-organized osteons with Haversian canals and interstitial lamellae. Abundant osteocytes with their characteristic processes in the canaliculi and their lacunae were obvious around the lased implants; Figure 3-C. The present results confirmed those of *Lopes et al., 2007 & Coelho et al., 2009.* ^(42,43) On contrast, other studies have shown that surfaces with different surface roughness may show a similar response with respect to cell adhesion and proliferation and the consequent development of mineralized tissue at their interface with the implant. ^(44,45)

The bone quality adjacent to the dental implant may provide valuable predictive information regarding implant performance. The bone implant contact percentage could be used as an indicator for the success of a dental implant at different implantation time ⁽⁴³⁾ such that a high percentage of bone contact would propose successful long-term stability. A histomorphometric analysis; (BIC%), of bone biopsies is a decisive assessment

method and the used computerized image analysis is an automated process yields more consistent results independent of the operator.

The percentage of bone contact depends on implant surface characteristics, local bone density, healing time, and loading time. ⁽⁴⁶⁾ The current results are in coincidence with *Orsini et al., 2000* ⁽⁴⁷⁾ who reported that CIB% exhibited a variation with different surface characteristics. The histomorphometric analysis guaranteed marked intimate interaction between tissues and implant surface of the experimental surface treated groups relative to the control one; Table 2 & Figure 4. As well, they confirmed those of *Klokkevold et al., 2001* ⁽⁴⁸⁾ where significantly higher bone-implant contact was observed for PIII implants compared to machined implants but significantly lower than those of laser surface treatment.

Analysis of the retrieved titanium implants showed that the bone-to implant contact is far from perfect, i.e. the osseointegration is incomplete. The bone-to-implant contact percentage averaged between 60%-80% even for successful implants that had lasted for up to 17 years. Both BIC% of PIII ($64.6 \pm 3.27\%$) and laser ($84.62 \pm 5.05\%$) specimens had fallen within the documented percentages. ⁽⁴⁹⁾ Bone grows both appositionally and through a matrix; the former process is slower ($0.6-1 \mu\text{m}/\text{day}$) than the later ($30-50 \mu\text{m}/\text{day}$). ⁽⁵⁰⁾ The collagen of the bone fibers might be in close proximity to the implant surface resulting in the significantly higher BIC% values of these treated groups. This could be referred to the substantial increase of surface energy due to charged nitrogen ion after plasma treatment. ^(51,52) As well, combining micro and nano topography due to laser ablation might be further reason for the intimate contact between mineralized bone tissues

and implant surface oxide as previously described by *Palmquist et al., 2010*. ⁽⁵³⁾

Lastly, it was reported that the osteoblast morphology varied according to the titanium surface texture and pattern. On polished surface with low surface roughness, cells are flat with scattered contact regions and they did not follow the orientation of parallel polishing lines. While over rough surfaces, osteoblasts are representing closer focal adhesion points. ⁽⁵⁴⁾ This was evidenced by the obtained results as a positive correlation could be established between surface roughness and CIB%. The surface of both prominent roughness and uniform pattern; Nd:YAG laser group, recorded the highest significant CIB%. On contrast, untreated control group displayed relatively plane surface and regular texture revealed the least CIB%.

CONCLUSIONS

It could be concluded that plasma immersion nitrogen ion implantation and Nd: YAG laser are effective physical surface modalities for Ti-implant alloys. They produced favor topographical texture and morphology that improved bone quality and quantity and provided better osseointegration.

REFERENCES

1. Oshida Y, Elif B, Tuna E, Aktören O, Gençay K. Dental Implant Systems. Int J Mol Sci.2010; 11:1580-1678.
2. Gittens R, McLachlan T, Navarrete O, et al. The effects of combined micron-/submicron-scale surface roughness and nanoscale features on cell proliferation and differentiation. Biomaterials.2011; 32: 3395–3403.
3. Conforto E, Caillard D, Aronsson BO, Descouts P. Electron microscopy on titanium implants for bone replacement after 'SLA' surface treatment. Eur Cells Mater.2002; 3:9-10.

4. Branemark P, Zarb G, Albrektsson T. Tissue Integrated Prostheses: Osseointegration in Clinical Dentistry. Chicago: Quintessence.1995; 11-76.
5. Listgarten M, Lang N, Schroeder H, Schroeder A. Periodontal tissues and their counterparts around endosseous implants. Clin Oral Impl Res.1991; 2:1-19.
6. Le Guehennec L, Soueidan A, Layrolle P, Amouriq Y. Surface treatments of titanium dental Implants for rapid osseointegration. Dent mater.2007; 23: 844–854.
7. Liu X, Chu P, Ding C. Surface modification of titanium, titanium alloys, and related materials for biomedical applications. Materials Science and Engineering Reports.2004; 47: 49-121.
8. Faeda R, Tavares H, Sartori R, Guastaldi A, Marcantonio E. Evaluation of titanium implants with surface modification by laser beam. Biomechanical study in rabbit tibias. Braz Oral Res.2009; 23:137-43
9. Tavakoli J, Khosroshahi ME, Mahmoudi M. Characterization of Nd: YAG laser radiation effects on Ti6Al4V physico-chemical properties: an in vivo study. Int.J.Eng. Transactions B: Appl. 2007; 20 (1): 1-11.
10. Götz H, Muller M, Emmel A, Erben R. Effect of surface finish on osseointegration of laser-treated titanium alloy implants. Biomater.2004; 25:4057-4064
11. Sakso M, Jakobsen S, Sakso H, Baas J. Acid etching and plasma sterilization fail to improve osseointegration of grit blasted titanium implants. Open Orthoped.2012; 6: 376-382
12. Hall L, Clarke K, Trim C. Principle of sedation, analgesia and premedication in veterinary anaesthesia 10th Ed. W.B. Saunders.2001; 79: 402-404.
13. Denny H, Butterworth S. The femur. A Guide to Canine and Feline Orthopedic Surgery, 4th ed. Blackwell Publishing Company.2000; pp. 495
14. Mavis B & Tas A. Dip coating of calcium hydroxyapatite on Ti-6Al-4V substrates. J Am Cer Society.2000; 83: 989–991.
15. Kuroda K, Moriyama M, Ichino R, Okido M, Seki A. Formation and osteoconductivity of hydroxyapatite/collagen composite films using a thermal substrate method in aqueous solutions. Mater Trans.2009; 50:1190–1195.
16. Kuroda K & Okido M. Hydroxyapatite coating of titanium implants using hydroprocessing and evaluation of their osteoconductivity. BioinorgChem Appl. 2012; doi: 10.1155/2012/730693. PMID:22400015:1-8.
17. Elias L, Schneider S, Silva H, Malvisi F. Microstructural and mechanical characterization of biomedical Ti–Nb–Zr-Ta alloys. Mater Sci Eng.2006; 432(1):108–12.
18. Puleo DA & Nanci A (1999). Understanding and controlling the bone-implant interface. Biomaterials.1999; 20: 2311-2321.
19. Chu P. Plasma surface treatment of artificial orthopedic and cardiovascular biomaterials. Surf Coat Technol.2007; 201: 5601–5606.
20. Asadinezhad A, Novak I, Lehocky M, et al. Irganon coating, Plasma Processes and Polymer.2010; 7 (6):504–514.
21. Liu F, Lia B, Sun J, Li H, Wang B, Zhang S. Proliferation and differentiation of osteoblastic cells on titanium modified by ammonia plasma immersion ion implantation. Applied surface science.2012; 258: 4322-4327.
22. Giro G, Tovar N, Witek L, Marin C, Silva N. Osseointegration assessment of chair side argon-based non thermal plasma treated Ca-P coated dental implants. J Biomed Mater Res.2012; Part A; 1-6
23. Ballo A, Omar O, Xia W, Palmquist A. Dental implant surfaces – physicochemical properties, biological performance and trends. 2011; Chapter 2, pp: 1-39.

24. Nayak S & Dahotre N. The laser induced combustion synthesis of iron oxide nanocomposite coating on aluminum. *J Miner Metals Mater Soc.*2002; 54: 39–41.
25. Shigematsu I, Nakamura M, Saitou N, Shimojima K. Surface hardening treatment of pure titanium by carbon dioxide laser. *J Mater Sci Lett.*2000; 19:967-970.
26. Itala A, Ylanen H, Ekholm C, Karlsson K, Aro H. Pore diameter of more than 100 μm is not requisite for bone ingrowth in rabbits. *J Biomed Mater Res.*2000; 58:679-83.
27. Gaggl A, Schultes G, MullerW, Karcher H. Scanning electron microscopical analysis of laser-treated titanium implant surfaces. A comparative study. *Biomater.*2000; 21: 1067-1073.
28. Cooper L, Masuda T, Yliheikkila P, Felton D. Generalization regarding the process and phenomenon of osseointegration Part 2: In vitro studies *J Oral Maxillofac Impla.*1998; 13:163-174.
29. Yan W, Nakamura T, Kobayashi M, Kim, Kokubo T. Bonding of chemically treated titanium implants to bone. *J Biomed Mater Res.*1997; 37:267-275.
30. Shalabi MM, Gortemaker A, Van't Hof MA, et al. Implant Surface Roughness and Bone Healing: a Systematic Review. *J Dent Res.*2006; 85(6):496-500.
31. Esposito M, Grusovin MG, Willings M, et al. Conventional Loading of Dental Implants: A Cochrane Systematic Review of Randomized Controlled Clinical Trials. *Int J Oral Maxillofac Implant.*2007; 22:893–904.
32. Brunski JB. In vivo bone response to biomechanical loading at the bone/dental-implant interface. *Adv Dent Res.*1999; 13: 99–119.
33. Wennerberg A, Albrektsson T, Albrektsson B, IJJ K. Histomorphometric and removal torque study of screw-shaped titanium implants with three different surface topographies. *Clin Oral Implant Res.*1996; 6:24–30.
34. Cho S. & Jung S. A removal torque of the laser treated titanium implants in rabbit tibia. *Biomater.*2003; 24: 4859-4863.
35. Skurla G, Pluhar D, Frankel E, Egger L. Assessing the dog as a model for human total hip replacement. *J Bone Joint Surg.*2005; 87:120-127.
36. Mendonça G, Mendonça D, Aragão F, Cooper L. Advancing dental implant surface technology from micron to nanotopography. *Biomater.*2008; 29: 3822–3835.
37. Ramazanoglu M. &Oshida Y. Osseointegration and bioscience of implants surfaces-current concepts at bone-implant interface. *Implant Dentistry- A rapidly Evolving Practice.* IlserTurkyilmazISBN 978-953-307-658-4, DOI: 10.5772/16936 (ed.) 2011; e- InTechBooks, Chapter 3; pp 57- 83.
38. Guo C, Matinlinna J. Effect of surface charges on dental implants: Past, present and future. *Inter J Biomater.*2012b; 1-5
39. García P, Prados-Sánchez E, Olmedo-Gaya V, et al. Measurement of dental implant stability by resonance frequency analysis: A review of the literature. *Med Oral Patol Oral Cir Bucal.*2009; 14: 538-546.
40. Davies J. Understanding peri-implant endosseous healing. *J Dent Educ.*2003; 67:932-949.
41. Suzuki K, Aoki K, Ohya K. Effects of Surface Roughness of Titanium Implants on Bone Remodeling Activity of Femur in Rabbits. *Bone.*1997; 21: 507-51
42. Lopes C, Pinherio A, Sathalah S, Silva N. Infrared laser photobiomodulation (830nm) on bone tissue around dental implants: A Raman spectroscopy and scanning electronic microscopy study in rabbits. *Photomed& Laser Surg.*2007; 25: 96-100.
43. Coelho P, Granjeiro J, Romanos G, et al. Basic research methods and current trends of dental implant surfaces. *J*

- Biomed Mater Res. Appl Biomater. 2009; 88:579-596.
44. Mustafa K, Wennerberg A, Worblewski J, et al. Determining the optimal surface roughness of Ti O₂ blasted titanium implant material for attachment, proliferation and differentiation of cells derived from human mandibular alveolar bone. *Clin Oral Imp Res.*2001; 12: 515-525.
 45. Huang H, Ho C, Lee T, Liao K. Effect of surface roughness of ground titanium on initial cell adhesion. *Biomol Eng.* 2004; 21:93-97.
 46. Tull L. Measuring bone density at distance lateral to the bone-implant interface with various stages of loading: A histomorphometric analysis in baboon. Master thesis.2003; pp: 23-46.
 47. Orsini G, Assenza B, Scarano A, et al. Surface analysis of machined versus sandblasted and acid-etched titanium implants. *Int J Oral Maxillofac Impl.* 2000; 15: 779-784.
 48. Klokkevold P, Johnson P, Dadgostari S. Early andosseous integration enhanced by dual acid etching of titanium: a torque removal study in the rabbit. *J Clin Oral Impl Res.*2001; 12: 350-357.
 49. Albrektsson T, Eriksson AR, Friberg B, et al. Histologic investigations on 33 retrieved Nobelpharma implants. *Clin Mater.*1993; 12:1-9.
 50. Davies JE & Hosseini MM. Histodynamics of endosseous wound healing. In *Bone Engineering.* (ed. JE Davies). Toronto, Canada: em squared Inc.2000; Chapter I, pp1-14.
 51. Hayashi M, Jimbo R, Lindh L, et al. In vitro characterization and osteoblast responses to nanostructured photocatalytic TiO₂ coated surfaces. *Acta Biomater.*2012; 8: 2411-2416.
 52. Guastaldi FPS, Yoo GD, Marin C, et al. Plasma Treatment Maintains Surface Energy of the Implant Surface and Enhances Osseointegration. *Int J of Biomat.* 2013; doi: 10.1155/2013/354125; PMID:23365578 [PubMed] PMCID: PMC3556447:1-6.
 53. Palmquist A, Engqvist H, Thomsen P. Biomechanical, histological and ultrastructural analyses of laser micro- and nano- structural titanium alloy implants: A study in rabbit. *J Biomed Mater Res.*2010; 92: 1476-1486.
 54. Silva J, Amico S, Neves A, Barboza C. Osteoblast like cell adhesion on titanium surfaces modified by plasma nitriding. *Int J Oral Maxillofac Implants.*2011; 26: 237-244.

How to cite this article: Eldadamony EM, Badr NA, Hegazy EM et. al. Efficiency of different physical surface modalities on osseointegration of titanium alloy implants. *Int J Health Sci Res.* 2015; 5(5):203-215.
